PERGAMON

Chemical Engineering Science 54 (1999) 4903–4911

Chemical Engineering Science

Influence of scale on the hydrodynamics of bubble columns operating in the churn-turbulent regime: experiments vs. Eulerian simulations

R. Krishna*, M.I. Urseanu, J.M. van Baten, J. Ellenberger

Department of Chemical Engineering, University of Amsterdam, Nieuwe Achtergracht 166, 1018 WV Amsterdam, The Netherlands

Abstract

The radial distribution of the liquid velocities, along with the liquid-phase axial dispersion coefficients, have been measured for the air–water system in bubble columns of 0.174, 0.38 and 0.63 m diameter. The experimental results emphasise the significant influence of the column diameter on the hydrodynamics, especially in the churn-turbulent regime. Computational fluid dynamics (CFD) is used to model the influence of column diameter on the hydrodynamics. The bubble column is considered to be made up of three phases: (1) liquid, (2) "small" bubbles and (3) "large" bubbles and the Eulerian description is used for each of these phases. Interactions between the gas phases and the liquid are taken into account in terms of momentum exchange, or drag, coefficients, which differ for these two gas phases. The drag coefficient between the small bubbles is estimated using the Harmathy correlation (*A.I.Ch.E.* Journal 6 (1960) 281–288). The drag relation for interactions between the large bubbles and the liquid, is developed from analysis of an extensive data base on large bubble swarm velocities measured in columns of 0.051, 0.1, 0.174, 0.19, 0.38 and 0.63 m diameter using a variety of liquids (water, paraffin oil, tetradecane). The interactions between the large and small bubble phases are ignored. The turbulence in the liquid phase is described using the k–ε model. The three-phase description of bubble columns was implemented within the Eulerian framework of a commercial code CFX 4.1c of AEA Technology, Harwell, UK. Comparison of the experimental measurements with the Eulerian simulations show good agreement and it is concluded that the three-phase Eulerian simulation approach developed here could be a powerful design and scale-up tool.

Keywords: Bubble columns; Large bubbles; Churn-turbulent flow regime; Radial velocity profiles; Column diameter influence; Computational fluid dynamics

1. Introduction

There is a considerable interest in developing reliable scale-up procedures for bubble column reactors operating in the churn-turbulent flow regime because of many industrial applications such as the Fischer–Tropsch synthesis of hydrocarbons (Krishna, Ellenberger & Sie, 1996; Krishna & Maretto, 1998). Bubble column reactors are invariably chosen as the reactor type for carrying out relatively slow liquid-phase reactions and where the liquid-phase backmixing is a desirable feature in order to achieve temperature equalization that is important for exothermic reactions. The radial distribution of liquid-phase velocities and the residence time distributions of the liquid phase are therefore important design parameters that need to be estimated. Though there is a considerable number of published papers in this area (see the comprehensive survey of literature references and correlations collected and presented on our web site: http://ct-cr4.chem.uva.nl/bc), there is a considerable difference in the predictions of these correlations, especially for large diameter columns.

The objectives of the present study are three-fold:

1. To generate a set of experimental data on the radial distribution of liquid velocities $V_L(r)$, in columns of varying diameters,
2. To measure the liquid-phase axial dispersion coefficient, $D_{ax,\,L}$ in the same columns under the same conditions so as to develop the proper inter-relationship between $D_{ax,\,L}$ and $V_L(r)$.
3. To develop a model to describe the scale dependence using computational fluid dynamics (CFD) in the Eulerian framework and compare the model predictions with experiment.

* Corresponding author. Tel.: +31-20-525-7007; fax: +31-20-5255604.

E-mail address: krishna@chemeng.chem.uva.nl (R. Krishna)

0009-2509/99/$ - see front matter
PII: S0009-2509(99)00211-0

2. Experimental

The axial component of the liquid velocities along the radial positions at different superficial gas velocities were measured using a modified Pitot tube, also called "Pavlov tube" (Hills, 1974), in three columns with different inner diameters: 0.174, 0.38 and 0.63 m. All three columns were made up of four polyacrylate sections with the total height of 4 m. In all three columns the pressure at the top corresponded to ambient conditions (101.3 kPa). A typical experimental set-up is shown in Fig. 1 for the 0.63 m bubble column. The columns were filled with demineralized water as liquid phase. The gas phase (air) was introduced at the bottom of the columns using different gas distributors. The 0.174 and 0.38 m diameter columns were equipped with sintered bronze plate gas distributors with an average pore size of 50 μm. The 0.63 m column was provided with a spider-shaped sparger, described in earlier work (Krishna & Ellenberger, 1996).

The Pavlov tube consists of a cylindrical tube placed across the column, through two diametrically opposed holes; see Fig. 2(a). The two 1 mm holes were drilled as close as possible to each other, ensuring that the liquid velocity was measured exactly at halfway distance between them. The radial liquid profiles were measured by moving the tube along the column radius. The two holes were placed in two different planes, perpendicular (orthogonal) to each other. A very thin diaphragm separated the interior of the tube in two sections, midway between the two holes. During operation of the column, bubbles can penetrate in the Pavlov tube, influencing the measurements. To minimize the disturbance of the measurements, a purge system was developed to remove the bubbles before each set of data acquisition. The short measuring time of 1 min that was chosen reduces the penetration chances of the bubbles into the tube. After purging the Pavlov tube the membrane must stabilize

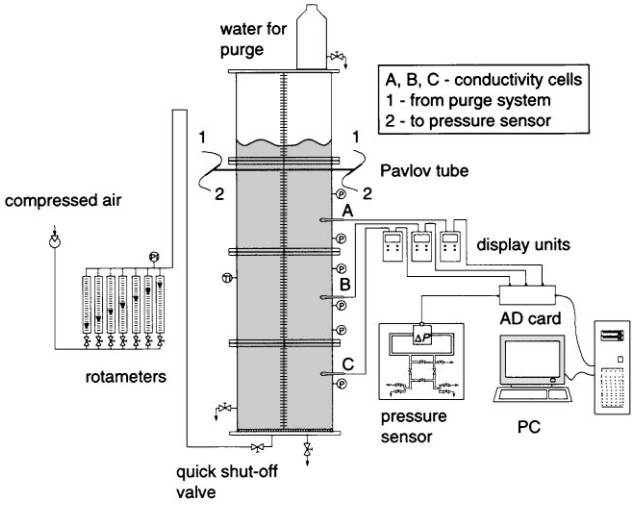

Fig. 1. Typical experimental set-up for 0.63 m diameter column.

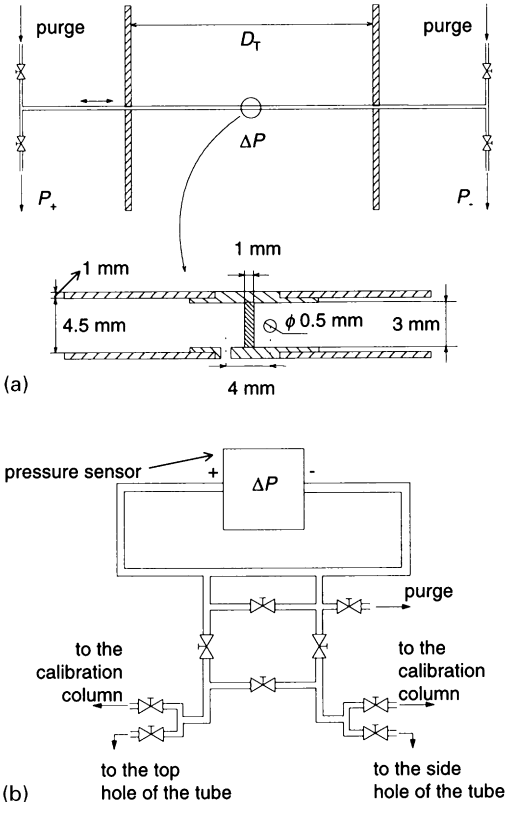

Fig. 2. Schematic diagram of (a) Pavlov tube and (b) differential pressure measuring system.

and therefore a waiting time of 30 s was allowed for before the next data acquisition was made. The extremities of the tube were connected with narrow PVC tubes to the measuring system (Fig. 2(b)). The complete measuring system consists of a pressure sensor (Validyne DP15 transducer), a display and a personal computer (see Fig. 1).

For determination of the liquid-phase residence time distribution a saturated solution of NaCl was used as a tracer. The solution was injected into the batch liquid phase as a pulse just above the dispersion height. Different volumes of tracer were used, depending on gas velocity, column diameter and injection position in order to obtain the optimal signal. In the 0.63 m diameter column the tracer was injected both in the middle and near the wall. For the remaining two columns, a single injection position was used, near the wall. The transient tracer concentration were monitored continuously by means of three Metrohm immersing-type conductivity cells which were placed near the wall, at different heights (A, B and C) as indicted in Fig. 1. Fig. 3 shows typical transient tracer concentrations for the 0.174 m diameter column; these signals were fitted using the analytic solution to the diffusion equation (Deckwer, 1992) to obtain a single value of the liquid-phase axial dispersion coefficient, $D_{ax,\,L}$ for a given experiment.

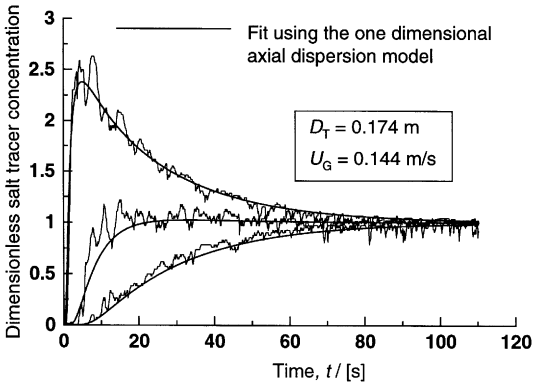

Fig. 3. Normalized liquid-phase tracer concentrations measured at three different locations along the height of the column in response to pulse tracer injection. The smooth curves represent the fits to the curves from fitting a diffusion model described in Deckwer (1992).

A detailed description of the experimental set-ups, data analysis of the signals from the Pavlov tube and electrical conductivity cells, along with the underlying theory are available on our website: http://ct-cr4.chem.uva.nl/bc.

3. Development of CFD model

Much attention has been paid in recent times to the use of CFD for the development of more fundamentally based models for simulating bubble column performance. A hierarchy of models exist for such simulations: (a) Eulerian – Eulerian model for the two, inter-penetrating, phases (Boisson & Malin, 1996; Grevskott, Sannaes, Dudukovic, Hjarbo & Svendsen, 1996; Grienberger & Hofmann, 1992; Jakobsen, Sannaes, Grevskott & Svendsen, 1997; Krishna, Van Baten & Ellenberger, 1998; Kumar, Vanderheyden, Devanthan, Padial, Dudukovic & Kashiwa, 1995; Lapin & Lübbert, 1994; Sokolichin & Eigenberger, 1994; Torvik & Svendsen, 1990), (b) Eulerian – Langrangian discrete bubble models (Delnoij, Lammers, Kuipers & van Swaaij, 1997a; Devanathan, Dudukovic, Lapin & Lübbert, 1995; Jakobsen et al., 1997; Sokolichin, Eigenberger, Lapin & Lübbert, 1997) and (c) the volume-of-fluid model (Delnoij, Kuipers & van Swaaij, 1997b; Hirt & Nichols, 1981; Krishna, Urseanu, van Baten & Ellenberger, 1999). From considerations of computer load, only the Eulerian – Eulerian two-phase model is suitable for the purpose of design and scale-up of industrial reactors. To use such Eulerian models for simulation of say the radial profiles of hold-ups and velocity at any position requires us to supply the appropriate momentum exchange, or drag, relations between the phases. For the homogeneous regime of operation of bubble columns, such drag relations can be found in the literature (Clift, Grace & weber, 1978). The situation with respect to the heterogeneous, or churn-turbulent, regime of operation is much more difficult because in this regime we have a roughly bi-modal distribution of bubble sizes: "small" and "large" (De Swart, Van Vliet & Krishna, 1996). The small bubbles are in the size range of 1 – 6 mm and are either spherical or ellipsoidal in shape depending on the physical properties of the liquid (Clift et al., 1978). The large bubbles are typically in the range of 20–80 mm range (De Swart et al., 1996) and fall into the spherical cap regime. These bubbles undergo frequent coalescence and break-up. The rise velocities of the large bubbles can approach 2 m/s and has been found to be significantly scale dependent (Krishna & Ellenberger, 1996). There are no available published correlations for the sizes of the large bubbles and their coefficients of momentum exchange (drag) with the liquid phase.

Kumar et al. (1995) attempted to simulate the experimental data of Hills (1974) data obtained in a 0.14 m diameter air–water bubble column operating at a superficial gas velocity $U = 0.169$ m/s by assuming that the entire bubble population has a uniform size of 3 mm. Though the agreement with the measured radial liquid velocity profile was good, they calculate much too high values of the gas hold-up. This is not unexpected because for air–water systems we would expect transition from homogeneous to heterogeneous regime to be at 0.034 m/s based on the estimation of the Reilly, Scott, De Bruijn, MacIntyre (1994) correlation and therefore at $U = 0.169$ m/s we would expect a significant proportion of the bubble population to be large and in the 20–80 mm size range.

We develop a CFD model for churn-turbulent operation of bubble columns in which we identify three phases: (1) liquid, (2) "small" bubbles and (3) "large" bubbles; see Fig. 4. This is the model used by us earlier to develop empirical correlations for the hold-ups (Krishna & Ellenberger, 1996). In conformity with the Krishna–Ellenberger model we assume that the superficial gas velocity through the small bubble phase corresponds to that at the regime transition point, U_{trans}; this velocity is

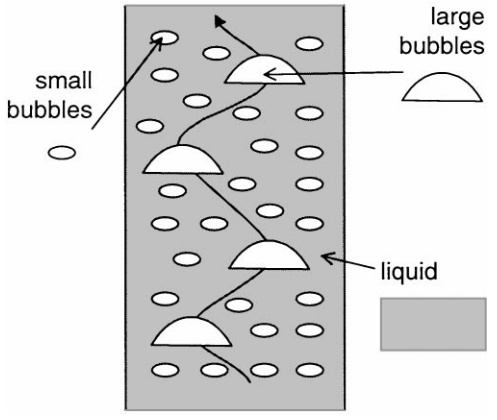

Fig. 4. Three-phase model for bubble columns operating in the churn-turbulent regime.

estimated using the Reilly et al. (1994) correlation. Each of the three phases is modelled within the Eulerian framework.

From visual observations of bubble column operations with the air–water system, the small bubbles were observed to be in the 3–6 mm size range. The rise velocity of air bubbles is practically independent of bubble diameter in this size range and the Harmathy (1960) equation for the rise velocity

$$V_{b,\,\mathrm{small}} = 1.53\,(\sigma g/\rho_L)^{0.25} \tag{1}$$

is used in the simulation model developed here.

In our earlier work (Krishna & Ellenberger, 1996) we had reported data on large bubble gas hold-up, $\varepsilon_{b,\,\mathrm{large}}$ in columns of 0.051, 0.1, 0.174, 0.19, 0.38 and 0.63 m using a variety of liquids (water, paraffin oil, tetradecane). The correlation developed in our earlier work for the large bubble hold-up cannot be readily used in CFD models, which require estimation of both the bubble sizes and the corresponding rise velocities. In order to develop this information we re-analysed our extensive data set in order to obtain a correlation for the rise velocity of a swarm of large bubbles in the form

$$V_{b,\,\mathrm{large}} = 0.71\sqrt{g d_{b,\mathrm{large}}}\,(\mathrm{SF})(\mathrm{AF}), \tag{2}$$

where we introduce two correction factors into the classical Davies–Taylor (Davies & Taylor, 1950) relation for the rise of a single spherical cap bubble in an infinite volume of liquid. Eq. (2) is valid for bubble sizes and system properties for which the Eötvös number, $E\ddot{o} > 40$ (see Clift et al., 1978). The scale correction factor (SF) accounts for the influence of the column diameter and is taken from the work of Collins (1967) to be

$$SF = \begin{cases} 1 & \text{for } d_{b,\mathrm{large}}/D_T < 0.125, \\ 1.13\exp(-d_{b,\mathrm{large}}/D_T) & \text{for } 0.125 < d_{b,\mathrm{large}}/D_T < 0.6, \\ 0.496\sqrt{D_T/d_{b,\mathrm{large}}} & \text{for } d_{b,\mathrm{large}}/D_T > 0.6. \end{cases} \tag{3}$$

The acceleration factor AF accounts for the increase in the large bubble velocity over that of a single, isolated, bubbles; this acceleration is due to wake interactions. This factor increases as the distance between the large bubbles decreases (Krishna et al., 1999). Since the average distance between large bubbles will decrease as the superficial gas velocity through the large bubble phase increases, we postulate a linear relation for AF:

$$\mathrm{AF} = \alpha + \beta(U - U_{\mathrm{trans}}) \tag{4}$$

and a power-law dependence of the bubble size on $(U - U_{\mathrm{trans}})$:

$$d_{b,\,\mathrm{large}} = \gamma(U - U_{\mathrm{trans}})^{\delta}. \tag{5}$$

The model parameters α, β, γ and δ were determined by multiple regression of the measured data on the rise velocity of large bubbles collected earlier in our laboratories and reported in Krishna and Ellenberger (1996). The fitted values are

$$\alpha = 2.73,\ \beta = 4.505,\ \gamma = 0.069,\ \delta = 0.376. \tag{6}$$

The bubble sizes calculated according to Eqs. (5) and (6) agree to within 20% with the measurements (De Swart et al., 1996) for the air–paraffin oil and air–water systems. It is also interesting to note that the acceleration factor AF varies between 3 and 6, stressing the strong influence of wake interactions on the bubble rise velocity. The complete fundamental background to the development of the expressions for the large bubble velocity, Eqs. (2)–(6), is available in a companion paper (Krishna et al., 1999).

For each of the three phases shown in Fig. 4, the volume-averaged mass and momentum conservation equations are given by

$$\frac{\partial(\varepsilon_k\rho_k)}{\partial t} + \nabla\cdot(\rho_k\varepsilon_k\mathbf{u}_k) = 0, \tag{7}$$

$$\frac{\partial(\rho_k\varepsilon_k\mathbf{u}_k)}{\partial t} + \nabla\cdot(\rho_k\varepsilon_k\mathbf{u}_k\mathbf{u}_k - \mu_k\varepsilon_k(\nabla\mathbf{u}_k + (\nabla\mathbf{u}_k)^T)) = -\varepsilon_k\nabla p + \mathbf{M}_{kl} + \rho_k\,\mathbf{g}, \tag{8}$$

where ρ_k, $\mathbf{u}_k$, ε_k and μ_k represent, respectively, the macroscopic density, velocity, volume fraction and viscosity of the kth phase, p is the pressure, $\mathbf{M}_{kl}$, the interphase momentum exchange between phase k and phase l and $\mathbf{g}$ is the gravitational force. The added mass force has been ignored in the present analysis. The reason for this neglect is that the concept of added mass is not applicable for the large bubbles, which do not have a closed wake. Furthermore, the focus of this paper is the modeling of the churn-turbulent flow regime wherein the gas holdups are high and there is evidence to suggest that the added mass coefficient decreases with increasing gas holdup (Jakobsen et al., 1997). Lift forces are also ignored in the present analysis because of the uncertainty in assigning values of the lift coefficients to the small and large bubbles. For the large bubbles, for which $E\ddot{o} > 40$ holds, literature data suggest the use of a negative lift coefficient, whereas for small bubbles for which typically $E\ddot{o} = 2$, the lift coefficient is positive. For the continuous, liquid, phase, the turbulent contribution to the stress tensor is evaluated by means of k–ε model, using standard single phase parameters $C_\mu = 0.09$, $C_{1\varepsilon} = 1.44$, $C_{2\varepsilon} = 1.92$, $\sigma_k = 1$ and $\sigma_\varepsilon = 1.3$. No turbulence model is used for calculating the velocity fields inside the dispersed "small" and "large" bubble phases. The momentum exchange between either bubble phase (subscript b) and liquid phase (subscript L) phases is given by

$$\mathbf{M}_{L,b} = \frac{3}{4}\,\rho_L\,\frac{\varepsilon_b}{d_b}\,C_D\,(\mathbf{u}_b - \mathbf{u}_L)|\mathbf{u}_b - \mathbf{u}_L|. \tag{9}$$

The liquid-phase exchanges momentum with both the "small" and "large" bubble phases. However, each of the dispersed bubble phases exchange momentum only with the liquid phase. The interphase drag coefficient is calculated from the equation

$$C_D = \frac{4}{3}\frac{\rho_L - \rho_G}{\rho_L} g d_b \frac{1}{V_b^2}, \tag{10}$$

where Eqs. (1) and (2) give the rise velocity of the bubbles, V_b, for the small and large bubble phases, respectively. The wake acceleration factor AF, the scale factor SF, and the bubble size d_b required in Eq. (2) are calculated using Eqs. (3)–(6).

A commercial CFD package CFX 4.1c of AEA Technology, Harwell, UK, was used to solve the equations of continuity and momentum for the two-fluid mixture. This package is a finite-volume solver, using body-fitted grids. The grids are non-staggered and all variables are evaluated at the cell centers. An improved version of the Rhie-Chow (1983) algorithm is used to calculate the velocity at the cell faces. The pressure–velocity coupling is obtained using the SIMPLEC algorithm (Van Doormal & Raithby, 1984). For the convective terms in Eqs. (7) and (8) hybrid differencing was used. A fully implicit backward differencing scheme was used for the time integration.

We simulated air–water operation in columns of 0.174, 0.38 and 0.63 m diameter for the superficial gas velocity range $U = 0.02$ to 0.35 m/s, using a total column height of 3 m. Axi-symmetry was assumed in the simulations using cylindrical coordinates. The same grid strategy used for all the columns. In the radial direction 30 grid cells were used, 10 grid cells in the central core and 20 grid cells towards the wall region. In the axial direction the first 0.2 m bottom portion of the column consisted of 10 mm cells and the remainder 2.8 m height consisted of 20 mm cells. The total number of cells was 4800. The initial liquid height used in the simulations of the three column diameters (0.174, 0.38 and 0.63 m) were either 1.8 m (for operation at $U > 0.16$ m/s) or 2 m (for operation at $U < 0.16$ m/s). From the Reilly et al. (1994) correlation it was determined that the superficial gas velocity at the regime transition point $U_{\text{trans}} = 0.034$ m/s. For operation at $U < 0.034$ m/s, homogeneous bubbly flow regime was taken to prevail. For operation at $U > 0.034$ m/s, the complete three-phase model was invoked. Following the model of Krishna and Ellenberger (1996), we assume that in the churn-turbulent flow regime the superficial gas velocity through the small bubble phase is $U_{\text{trans}} = 0.034$ m/s. The remainder of the gas $(U - U_{\text{trans}})$ was taken to rise up the column in the form of large bubbles. This implies that at the distributor the "large" bubbles constitute a fraction $(U - U_{\text{trans}})/U$ of the total incoming volumetric flow, whereas the "small" bubble constitute a fraction (U_{trans}/U) of the total incoming flow. A further assumption made is that the formation of the large bubbles takes place immediately at the distributor; this is essentially a simplification and the justification for this is that our experimental studies show that the "large" bubbles equilibrate within a distance of 0.1 m above the distributor (Ellenberger & Krishna, 1994). The diameter of the "small" bubbles was chosen to be 4 mm in all the simulations and the drag coefficient determined from Eqs. (1) and (10). The large bubble size and drag coefficient was determined from Eqs. (2)–(6) and (10). The injection of the small bubble phase was uniformly done over the central 24 of the 30 bottom grid cells. Based on visual observations of bubble column operation in the churn-turbulent flow regime, the large bubbles tend to concentrate in the central core. In order to reflect this the large bubble phase was injected over the central 13 of the 30 grid cells. To test the sensitivity of the results to assumption of the regime transition velocity, simulations were also carried out taking $U_{\text{trans}} = 0.045$ m/s. The time-stepping strategy used in the transient simulations for attainment of steady state was: 20 steps at 5×10^{-4} s, 20 steps at 1×10^{-3} s, 460 steps at 5×10^{-3} s, 2000 steps at 1×10^{-2} s. The 0.174, 0.38 and 0.63 m diameter column simulations were carried out on a Silicon Graphics Power Indigo workstation with the R8000 processor. Each simulation was completed in about 36 h. In all the runs steady state was reached within 2500 time steps.

We also carried out simulations of an air–water bubble column of 0.14 m diameter and 1.3 m height for the superficial gas velocities $U = 0.019$, 0.038, 0.064, 0.095 and 0.169 m/s, corresponding to the experimental conditions of Hills (1974). In the radial direction, 30 grid cells were used, 10 grid cells in the central core and 20 grid cells towards the wall region. In the axial direction the bottom 0.2 m portion of the column consisted of 5 mm cells and the remainder 1.1 m height consisted of 10 mm cells. A total of $30 \times 150 = 4500$ grid cells were used. The operations at $U = 0.019$ and 0.038 m/s were both modeled as being in the homogeneous bubbly flow regime; the system was considered to be made up of only two phases: "small" bubbles and liquid. The complete three-phase model was invoked for operation at $U = 0.064$, 0.095 and 0.169 m/s. The initial liquid height used in the simulations was 0.9 m.

Further details of the Eulerian simulations, including animations of the column start-up dynamics are available on our web site: http://ct-cr4.chem.uva.nl/euler2D.

4. Simulations vs. experiments

Fig. 5 compares the simulation results for (a) total gas hold-up in 0.174 m column, (b) large bubble hold-up in 0.38 m column and (c) small bubble hold-up in 0.63 m column with experimental data of Krishna and Ellenberger (1996) obtained by the dynamic gas disengagement

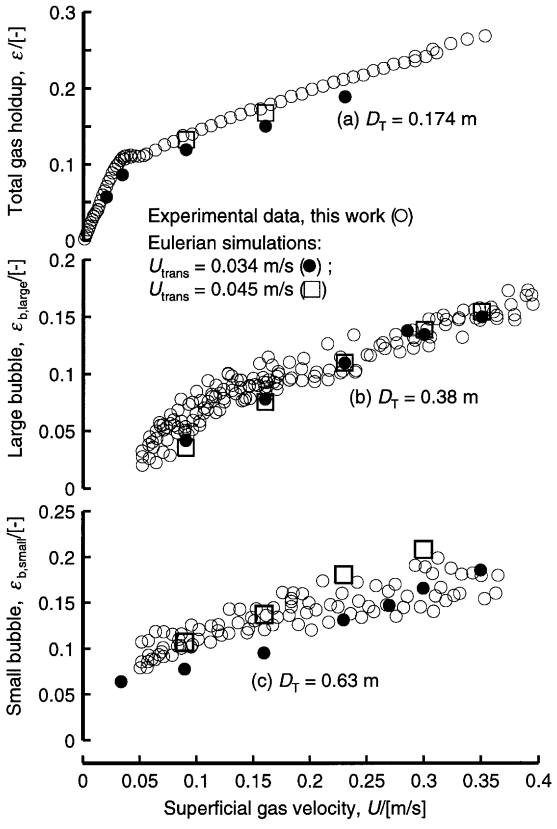

Fig. 5. (a) Total gas hold-up in 0.174 m diameter column. (b) Large bubble gas hold-up in 0.38 m diameter column. (c) Small bubble hold-up in 0.63 m diameter column. The experimental data are compared with Eulerian simulations carried out with two different values for U_{trans}: 0.034 and 0.045 m/s. The simulated values of the gas hold-up were determined by averaging the radial hold-up profile over the column cross section at a height of 1.6 m above the distributor.

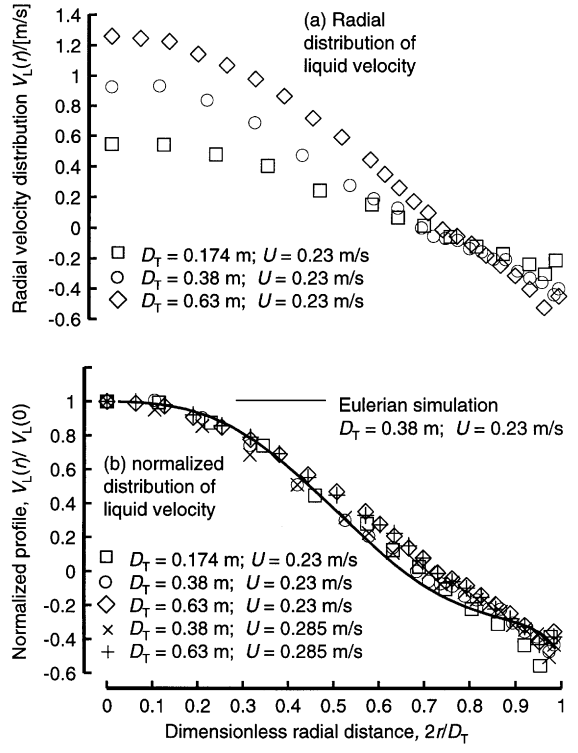

Fig. 6. (a) Radial distribution of the axial component of the liquid velocity at a superficial gas velocity of 0.23 m/s for three column diameters. (b) Normalized radial velocity distribution profile. The normalized profile for Eulerian simulation for $U = 0.23$ m/s and $D_T = 0.38$ m is also plotted; the other simulated profiles bunch around this profile very closely.

technique. The first point to note is that the simulations reproduce the right trend in the gas hold-ups with increasing gas velocity. The large bubble gas hold-up is not particularly sensitive to the assumption made with respect to the transition gas velocity U_{trans}; see Fig. 5(b). On the other hand, the small bubble hold-up is quite sensitive to the value chosen for U_{trans}; see Fig. 5(c). It appears that the experimental data of Krishna and Ellenberger (1996) are better represented by $U_{trans} = 0.045$ m/s. The total gas hold-up with the assumption $U_{trans} = 0.045$ m/s represents the experimental data very well; see Fig. 5(a). The importance of predicting the transition gas velocity with good accuracy is underlined by the comparisons presented in Fig. 5.

Fig. 6(a) shows the measured radial liquid velocity distribution for the three columns operating at a superficial gas velocity of 0.23 m/s. The strong influence of the column diameter on the liquid velocity is evident. If the data is normalized with respect to the centreline velocity, $V_L(0)$ we see that the radial distributions are all similar; see Fig. 6(b). Also shown in Fig. 6(b) is the normalized velocity distribution from the three-phase Eulerian simulation for $U = 0.23$ m/s and $D_T = 0.38$ m. The agreement is reasonably good. Similar good agreement is found when comparing our measured centreline liquid velocities with the results of Eulerian simulations; see Fig. 7. A further point to note from the simulation results of Fig. 7 is that simulation values for $V_L(0)$ is relatively insensitive to the choice of U_{trans} in the range of 0.034 and 0.045 m/s; this is in sharp contrast with the observed sensitivity of the small bubble hold-up to this choice. Also shown in Fig. 7 are two correlations for the centre line velocity from the literature, due to Riquarts (1981):

$$V_L(0) = 0.21(gD_T)^{1/2}(U^3\rho_L/g\mu_L)^{1/8} \quad (11)$$

and Zehner (1986):

$$V_L(0) = 0.737(UgD_T)^{1/3}. \quad (12)$$

From Fig. 7 we can conclude that our three-phase Eulerian simulations are comparable in accuracy with empirical correlations for estimating $V_L(0)$.

Figs. 8 and 9 compare the radial liquid velocity profiles and gas hold-ups measured by Hills (1974) with the results of our Eulerian simulations. Though the agreement can be considered to be reasonably good, we note

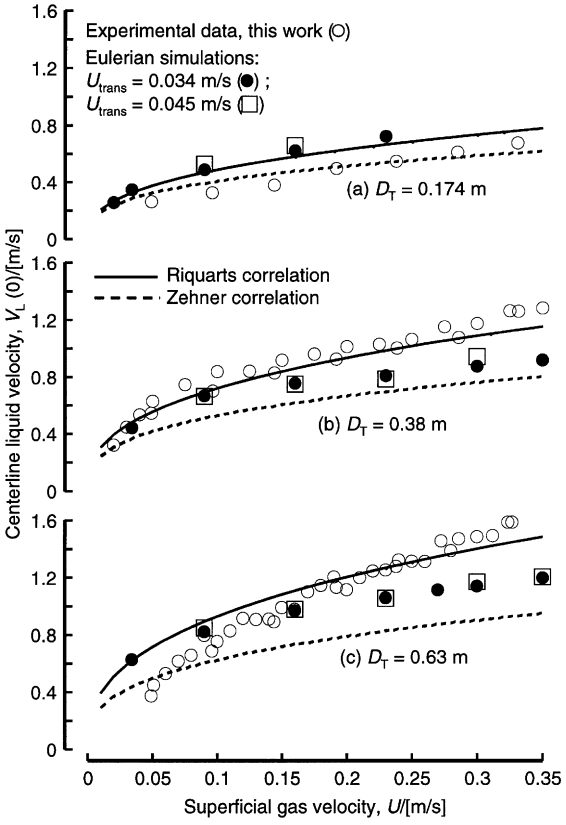

Fig. 7. Comparison between measured centreline liquid velocity $V_L(0)$ with those from Eulerian simulations carried out with two different values for U_{trans}: 0.034 and 0.045 m/s. Also shown are the empirical correlations of Riquarts (1981) and Zehner (1986). The simulated values of $V_L(0)$ were determined at a height of 1.6 m above the distributor.

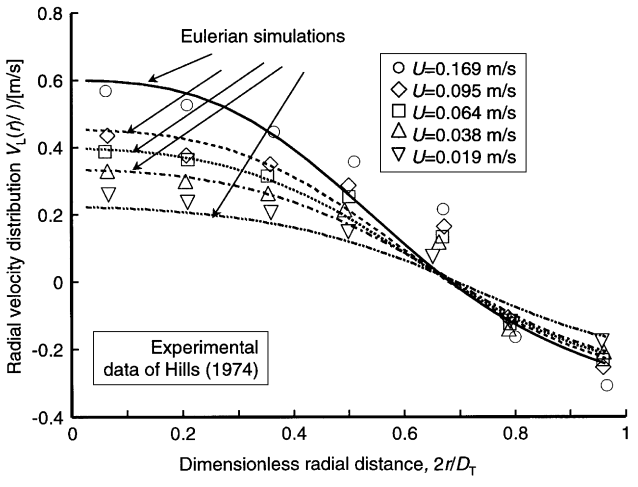

Fig. 8. Radial distribution of liquid velocities at a height of 0.6 m above the distributor. Comparison between Eulerian simulations with experimental data of Hills (1974). The simulated values of $V_L(r)$ were determined at a height of 0.6 m above the distributor.

that the simulations tend to overestimate the centreline liquid velocity, while underestimating the gas hold-up. Also shown in Fig. 9 are simulation results in which the

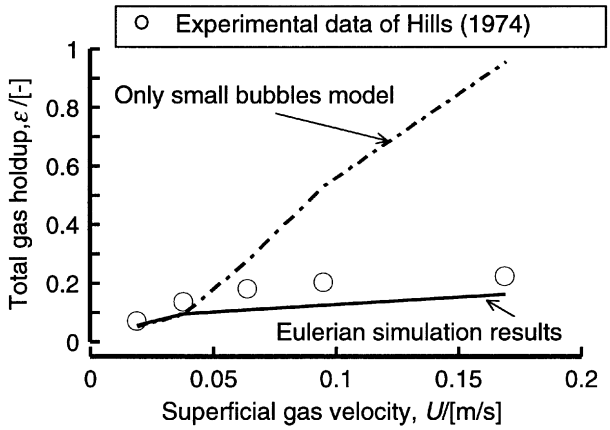

Fig. 9. Comparison of experimental data of Hills (1974) for total gas hold-up comparison with Eulerian simulations for a range of superficial gas velocities: U = 0.019, 0.038, 064, 0.095 and 0.169 m/s. Also shown with dotted line are simulation results in which the dispersion is assumed to consist only of 4 mm sized small bubbles. The simulated values of the gas hold-up were determined by averaging the radial hold-up profile over the column cross section at a height of 0.6 m above the distributor.

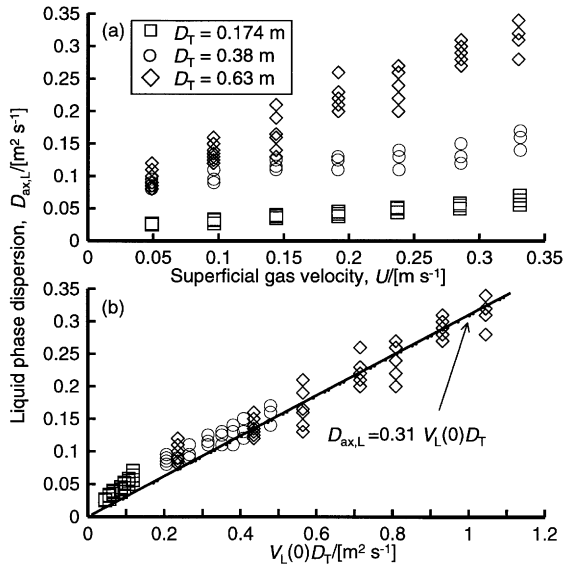

Fig. 10. Axial dispersion coefficient of the liquid phase: (a) $D_{ax,\,L}$ as a function of the superficial gas velocity. (b) $D_{ax,\,L}$ as a function of $V_L(0)D_T$.

gas dispersion is assumed to be made up of only small bubbles of 4 mm in diameter. The total gas hold-up is significantly higher than the experimental values, emphasizing the need for recognizing the existence of fast-rising large bubbles.

Our measurements of the axial dispersion coefficients for the liquid phase is seen to be a strong function of the column diameter; see Fig. 10(a). The experimental data $D_{ax,\,L}$ is seen to be simply proportional to the product of the centreline liquid velocity and the column diameter,

see Fig. 10(b). There is no need to set up a separate correlation for $D_{ax,\,L}$ as is done in the literature (see the survey of correlations presented on our web site: http://ct-cr4.chem.uva.nl/bc). Our suggestion is to use Eulerian simulations to estimate the centreline velocity $V_L(0)$ and estimate the axial dispersion coefficient from

$$D_{ax,\,L} = 0.31 V_L(0)\, D_T. \tag{13}$$

5. Conclusions

Both our experimental measurements and CFD simulations show that the column diameter has a significant influence on the magnitude of the centreline liquid velocity; see Fig. 7.

Our three-phase Eulerian simulations are in reasonable agreement with experimental results on centreline liquid velocity (Fig. 7), radial distribution of liquid velocity (Figs. 6 and 8), total gas hold-up (Fig. 5(a) and Fig. 9), large bubble gas hold-up (Fig. 5(b)), and small bubble hold-up (Fig. 5(c)). If we assume that the dispersion is formed only of small bubbles, the total gas hold-up is significantly overestimated; cf. Fig. 9.

The measurements on the axial dispersion coefficient in the liquid phase shows that this parameter is simply proportional to the product of the centreline liquid velocity and the column diameter; cf. Eq. (13).

On the basis of the promising results obtained in this paper we conclude that three-phase Eulerian simulations can be a powerful design and scale-up tool. However, an important assumption made in our model is that there is no interaction or exchange between the small and large bubble populations. This assumption will require testing in the future.

Notation

AF	acceleration factor, m/s
C_D	drag coefficient, dimensionless
d_b	diameter of either bubble population, m
$D_{ax,\,L}$	axial dispersion coefficient of the liquid phase, m^2/s
D_T	column diameter, m
$E\ddot{o}$	Eötvös number, $g(\rho_L - \rho_G)d_b^2/\sigma$
g	acceleration due to gravity, 9.81 m/s^2
H	dispersion height, m
M	interphase momentum exchange term
p	pressure, N/m^2
r	radial coordinate, m
SF	scale correction factor, dimensionless
t	time, s
u	velocity vector, m/s
U	superficial gas velocity, m/s
V_b	rise velocity of bubble population, m/s
$V_L(r)$	radial distribution of liquid velocity, m/s
$V_L(0)$	centreline liquid velocity, m/s

Greek letters

$\alpha, \beta, \gamma, \delta$	parameters defined by Eqs. (4)–(6)
ε	volume fraction of gas phase, dimensionless
$\varepsilon(r)$	radial distribution of total gas hold-up, dimensionless
$\varepsilon(0)$	centreline total gas hold-up, dimensionless
μ	viscosity of phase, Pa s
ρ	density of phases, kg/m^3
σ	surface tension of liquid phase, N/m
τ	stress tensor, N/m^2

Subscripts

b	referring to either bubble population
large	referring to the large bubble population
small	referring to the small bubble population
G	referring to gas phase
k	index referring to one of the three phases
L	referring to liquid phase
T	tower or column

References

Boisson, N., & Malin, M. R. (1996). Numerical prediction of two-phase flow in bubble columns. *International Journal of Numerical Methods in Fluids*, *23*, 1289–1310.

Clift, R., Grace, J. R., & Weber, M. E. (1978). *Bubbles, drops and particles*. San Diego: Academic Press.

Collins, R. (1967). The effect of a containing cylindrical boundary on the velocity of a large gas bubble in a liquid. *Journal of Fluid Mechanics*, *28*, 97–112.

Davies, R. M., & Taylor, G. I. (1950). The mechanics of large bubbles rising through extended liquids and through liquids in tubes. *Proceeding of the Royal Society of London*, *A200*, 375–390.

Deckwer, W. D. (1992). *Bubble column reactors*. New York: Wiley.

Delnoij, E., Lammers, F. A., Kuipers, J. A. M., & van Swaaij, W. P. M. (1997a). Dynamic simulation of dispersed gas-liquid two-phase flow using a discreet bubble model. *Chemical Engineering Science*, *52*, 1429–1458.

Delnoij, E., Kuipers, J. A. M., & van Swaaij, W. P. M. (1997b). Computational fluid dynamics applied to gas-liquid contactors. *Chemical Engineering Science*, *52*, 3623–3638.

De Swart, J. W. A., Van Vliet, R. E., & Krishna, R. (1996). Size, structure and dynamics of "large" bubbles in a 2-D slurry bubble column. *Chemical Engineering Science*, *51*, 4619–4629.

Devanathan, N., Dudukovic, M. P., Lapin, A., & Lübbert, A. (1995). Chaotic flow in bubble column reactors. *Chemical Engineering Science*, *50*, 2661–2667.

Ellenberger, J., & Krishna, R. (1994). A Unified Approach to the scaleup of gas-solid fluidized and gas-liquid bubble column reactors. *Chemical Engineering Science*, *49*, 5391–5411.

Grevskott, S., Sannæs, B. H., Dudukovic, M. P., Hjarbo, K. W., & Svendsen, H. F. (1996). Liquid circulation, bubble size distributions, and

solids movement in two- and three-phase bubble columns. *Chemical Engineering Science*, *51*, 1703–1713.

Grienberger, J., & Hofmann, H. (1992). Investigations and modelling of bubble columns. *Chemical Engineering Science*, *47*, 2215–2220.

Harmathy, T. J. (1960). Velocity of large drops and bubbles in media of infinite or restricted extent. *A.I.Ch.E.Journal*, *6*, 281–288.

Hills, J. H. (1974). Radial non-uniformity of velocity and voidage in a bubble column. *Transactions of the Insitutation of Chemical Engineers*, *52*, 1–9.

Hirt, C. W., & Nichols, B. D. (1981). Volume of fluid (VOF) method for the dynamics of free boundaries. *Journal of Computational Physics*, *39*, 201–225.

Jakobsen, H. A., Sannæs, B. H., Grevskott, S., & Svendsen, H. F. (1997). Modeling of bubble driven vertical flows. *Industrial and Engineering Chemistry Research*, *36*, 4052–4074.

Krishna, R., & Ellenberger, J. (1996). Gas holdup in bubble column reactors operating in the churn-turbulent flow regime. *A.I.Ch.E.Journal*, *42*, 2627–2634.

Krishna, R., Ellenberger, J., & Sie, S. T. (1996). Reactor development for conversion of natural gas to liquid fuels: A scale up strategy relying on hydrodynamic analogies. *Chemical Engineering Science*, *51*, 2041–2050.

Krishna, R., & Maretto, C. (1998). Scale up of a bubble column slurry reactor for fischer tropsch synthesis. Natural gas conversion V. In A. Parmaliana, et al., *Studies in surface science and catalysis*, vol. 119 (pp. 197–202). Amsterdam: Elsevier.

Krishna, R., van Baten, J. M., & Ellenberger, J. (1998). Scale effects in fluidized multiphase reactors. *Powder Technology*, *100*, 137–146.

Krishna, R., Urseanu, M. I., van Baten, J. M., & Ellenberger, J. (1999). Rise velocity of a swarm of large gas bubbles in liquids. *Chemical Engineering Science*, *54*, 171–183.

Kumar, S., Vanderheyden, W. B., Devanathan, N., Padial, N. T., Dudukovic, M. P. & Kashiwa, B. A. (1995). Numerical simulation and experimental verification of gas-liquid flow in bubble columns. In *Industrial mixing fundamentals with applications, A.I.Ch.E. Symposium Series No. 305*, vol 91, (pp. 11–19).

Lapin, A., & Lübbert, A. (1994). Numerical simulation of the dynamics of two-phase gas–liquid flows in bubble columns. *Chemical Engineering Science*, *49*, 3661–3674.

Reilly, I. G., Scott, D. S., De Bruijn, T. J. W., & MacIntyre, D. (1994). The role of gas phase momentum in determining gas holdup and hydrodynamic flow regimes in bubble column operations. *Canadian Journal of Chemical Engineering*, *72*, 3–12.

Rhie, C. M., & Chow, W. L. (1983). Numerical study of the turbulent flow past an airfoil with trailing edge separation. *AIAA Journal*, *21*, 1525–1532.

Riquarts, H. P. (1981). A physical model for axial mixing of the liquid phase for heterogeneous flow regime in bubble columns. *German Chemical Engineering*, *4*, 18–23.

Sokolichin, A., & Eigenberger, G. (1994). Gas-liquid flow in bubble columns and loop reactors: Part I. Detailed modelling and numerical simulation. *Chemical Engineering Science*, *49*, 5735–5746.

Sokolichin, A., Eigenberger, G., Lapin, A., & Lübbert, A. (1997). Direct numerical simulation of gas-liquid two-phase flows. Euler/Euler versus Euler/Lagrange. *Chemical Engineering Science*, *52*, 611–626.

Torvik, R., & Svendsen, H. F. (1990). Modelling of slurry reactors. A fundamental approach. *Chemical Engineering Science*, *45*, 2325–2332.

Van Doormal, J., & Raithby, G. D. (1984). Enhancement of the SIMPLE method for predicting incompressible flows. *Numerical Heat Transfer*, *7*, 147–163.

Zehner, P. (1986). Momentum, mass and heat transfer in bubble columns. Part 1. Flow model of the bubble column and liquid velocities. *International Chemical Engineering*, *26*, 22–35.